

# Probes for Detection of Specific DNA Sequences at the Single-Molecule Level

Jens-Peter Knemeyer, Nicole Marmé, and Markus Sauer\*

Physikalisch-Chemisches Institut, Universität Heidelberg, Im Neuenheimer Feld 253, 69120 Heidelberg, Germany

**A method has been developed for highly sensitive detection of specific DNA sequences in a homogeneous assay using labeled oligonucleotide molecules in combination with single-molecule photon burst counting and identification. The fluorescently labeled oligonucleotides are called smart probes because they report the presence of complementary target sequences by a strong increase in fluorescence intensity. The smart probes consist of a fluorescent dye attached at the terminus of a hairpin oligonucleotide. The presented technique takes advantage of the fact that the used oxazine dye JA242 is efficiently quenched by complementary guanosine residues. Upon specific hybridization to the target DNA, the smart probe undergoes a conformational change that forces the fluorescent dye and the guanosine residues apart, thereby increasing the fluorescence intensity about six fold in ensemble measurements. To increase the detection sensitivity below the nanomolar range, a confocal fluorescence microscope was used to observe the fluorescence bursts from individual smart probes in the presence and absence of target DNA as they passed through the focused laser beam. Smart probes were excited by a pulsed diode laser emitting at 635 nm with a repetition rate of 64 MHz. Each fluorescence burst was identified by three independent parameters: (a) the burst size, (b) the burst duration, and (c) the fluorescence lifetime. Through the use of this multiparameter analysis, higher discrimination accuracies between smart probes and hybridized probe–target duplexes were achieved. The presented multiparameter detection technique permits the identification of picomolar target DNA concentrations in a homogeneous assay, i.e., the detection of specific DNA sequences in a 200-fold excess of labeled probe molecules.**

High-sensitivity detection methods are increasingly important in many fields, such as environmental studies; health care, for example, early-stage diagnosis of a viral or bacterial infection; and basic physical and biochemical research.<sup>1–5</sup> For DNA detection, most methods use the polymerase chain reaction (PCR) to

increase the concentration of target sequence prior to analysis. To determine the presence of a specific DNA sequence, it is necessary to hybridize fluorescently labeled oligonucleotide probes and immobilize the hybrids on a solid surface.<sup>6,7</sup> After removal of the unhybridized probes, with a washing step, the remaining fluorescence intensity is measured. Unfortunately, the requirement that unhybridized probe molecules have to be removed precludes the use of this technique for on-line monitoring of hybridization. In addition, the physical separation of unhybridized probe molecules in a heterogeneous assay decreases the sensitivity due to nonspecific binding of probe molecules on the surface. Therefore, homogeneous assays using fluorescently labeled oligonucleotides are a desirable alternative.

Using fluorescence correlation spectroscopy (FCS) in combination with confocal fluorescence microscopy, the hybridization kinetics of fluorescently labeled oligonucleotides to target DNA<sup>8</sup> and the cleavage of M13DNA by several restriction enzymes has been successfully analyzed.<sup>9</sup> Eigen and co-workers<sup>10</sup> have demonstrated the identification of HIV-1 RNA by FCS with the help of a complementary fluorescent primer. Since the sensitivity of FCS affords nanomolar concentrations,<sup>11</sup> the virus RNA, which is present at a very low level ( $\sim 10^{-18}$  M) in blood plasma, has been amplified using nucleic acid sequence-based amplification (NASBA) prior to the hybridization measurements. However, to secure hybridization of the labeled oligonucleotide to the target sequence in more dilute solutions ( $< 10^{-10}$  M), relatively high concentrations of labeled oligonucleotides have to be used. Thus, the large excess of free labeled oligonucleotide molecules which exhibit unchanged physical properties complicates or even prevents the detection of a few positive signals. On the other hand, by using two-color detection in combination with two differently labeled nucleic acid probes complementary to different sites on the target DNA, an homogeneous assay can be performed in the concentration range below  $10^{-10}$  M. This approach has been successfully used to detect specific nucleic acid sequences in unamplified genomic DNA.<sup>12</sup>

\* Corresponding author: (phone) (49)-6221-548460; (fax) (49)-6221-544255; (e-mail) sauer@urz.uni-heidelberg.de.

(1) Eigen, M.; Rigler, R. *Proc. Natl. Acad. Sci. U.S.A.* **1994**, *91*, 5740–5747.  
(2) Haab, B. B.; Mathies, R. A. *Anal. Chem.* **1995**, *67*, 3253–3260.  
(3) Castro, A.; Shera, E. B. *Anal. Chem.* **1995**, *67*, 3181–3186.  
(4) Weiss, S. *Science (Washington, D.C.)* **1999**, *283*, 1676–1683.  
(5) Kim, Y.; Jett, J. H.; Larson, E. J.; Pentilla, J. R.; Marrone, B. L.; Keller, R. A. *Cytometry* **1999**, *36*, 324–332.

(6) Ausubel, F. M.; Brent, R.; Kingston, R. E.; Moore, D. D.; Seidman, J. G.; Smith, J. A.; Struhl, K. *Current Protocols in Molecular Biology*; John Wiley & Sons: New York, 1994.  
(7) Chehab, F. F.; Kann, Y. W. *Proc. Natl. Acad. Sci. U.S.A.* **1989**, *86*, 9178–9182.  
(8) Schwillie, P.; Oehlenschläger, F.; Walter, N. G. *Biochemistry* **1996**, *35*, 10182.  
(9) Kinjo, M.; Nishimura, G.; Koyama, T.; Mets, Ü.; Rigler, R. *Anal. Biochem.* **1998**, *260*, 166–172.  
(10) Oehlenschläger, F.; Schwillie, P.; Eigen, M. *Proc. Natl. Acad. Sci. U.S.A.* **1996**, *93*, 12811–12816.  
(11) Maiti, S.; Haupts, U.; Webb, W. W. *Proc. Natl. Acad. Sci. U.S.A.* **1997**, *94*, 11753–11757.

3'-TTTATCATCAAGGAGTGTCCCTTA-5'

Target DNA

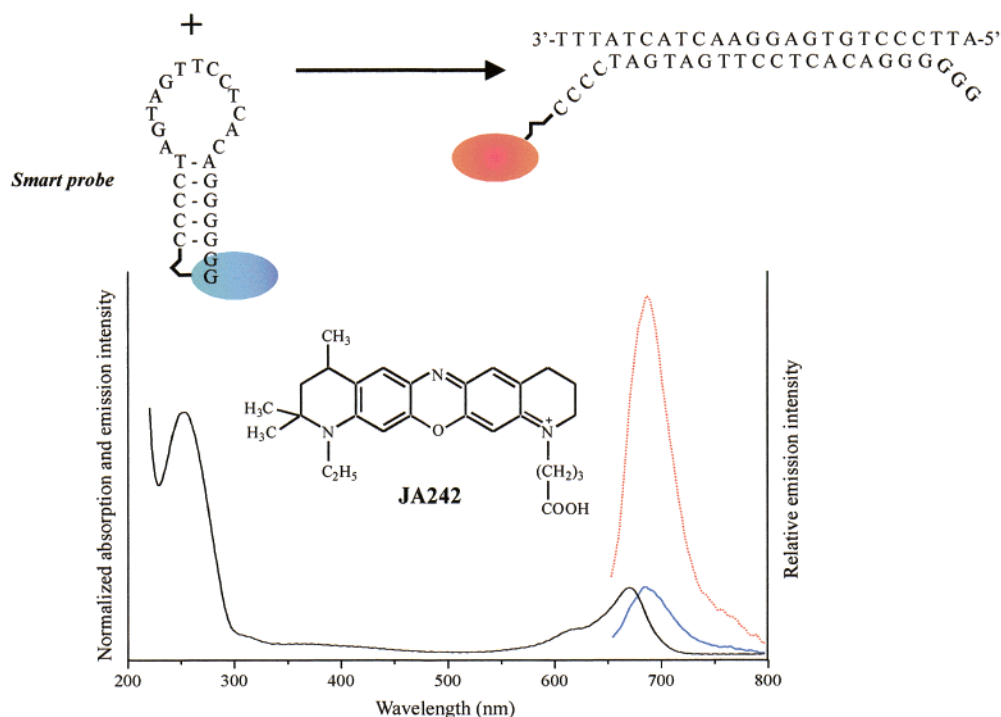


Figure 1. Working mechanism of smart probes and molecular structure of the used oxazine dye JA242. The complementary guanosine residues in the closed hairpin structure cause strong fluorescence quenching of the oxazine dye. Upon addition of an excess of target sequence and subsequent hybridization to the target the interaction between the dye and the guanosine residues is interrupted and the fluorescence released. In addition, the normalized absorption and emission spectra of the closed smart probe (---) and the relative emission spectrum of the hybridized smart probe (---) in 100 mM tris-borate buffer (pH 7.4) containing 140 mM NaCl and 5 mM MgCl<sub>2</sub> are given.

Recently,<sup>13,14</sup> Tyagi and Kramer introduced hairpin-shaped oligonucleotide probes that report the presence of specific nucleic acids by a strong increase in fluorescence intensity. These so-called Molecular Beacons are single-stranded nucleic acid molecules that possess a stem-loop structure and are ideally suited for highly sensitive homogeneous DNA binding assays. The loop consists of a probe sequence that is complementary to a sequence in the target, whereas the stem is formed by annealing of two complementary arm sequences which are unrelated to the target sequence. The hairpin oligonucleotide is labeled with a fluorescent dye at the 5' position and another chromophore at the 3' terminus. Upon close contact of both chromophores, fluorescence resonance energy transfer (FRET) occurs, i.e., the closed-hairpin oligonucleotide is strongly quenched. When the hairpin probe encounters a target molecule, it forms a longer and more stable hybrid than that formed by the arm sequences. Consequently, the molecular beacon undergoes a conformational change that forces the FRET donor and acceptor apart, thereby increasing the measured fluorescence intensity of the donor about 25-fold. This property has been used to demonstrate allele discrimination<sup>15</sup> and spectral genotyping<sup>16</sup> in ensemble measurements at the micromolar level. However, the specific labeling of both termini of molecular beacons with different fluorophores is difficult and delivers only

small yields per reaction. Furthermore, if the oligonucleotide is labeled only with the donor dye, highly sensitive assays are complicated due to unquenched probe molecules.

In this paper we present the design and application of new hairpin-shaped oligonucleotide probe molecules for homogeneous assays at the single-molecule level (nano- to picomole range). The new probes also consist of a stem-loop structure that is released upon specific hybridization to the target sequence. In contrast to the molecular beacons, our hairpin oligonucleotide probes are only labeled at one end with a fluorescent dye. Hence, unlabeled oligonucleotides do not contribute to the measured signal. Since the used fluorescent dye recognizes its microenvironment, i.e., the DNA sequence in the immediate neighborhood, we call our labeled oligonucleotide probes "Smart Probes". To reduce the background due to autofluorescence of the sample, we used one of the recently developed oxazine derivatives as the fluorescent label, which absorbs and emits in the red wavelength range (630–700 nm).<sup>17,18</sup>

## MATERIALS AND METHODS

**Sample Preparation and Spectroscopy.** All experiments were performed with the new oxazine dye JA242 (Figure 2).<sup>18</sup> Details of dye preparation are given in ref 19. The oligonucleotides

(12) Castro, A.; Williams, J. G. K. *Anal. Chem.* **1997**, *69*, 3915–3920.

(13) Tyagi, S.; Kramer, F. R. *Nat. Biotechnol.* **1996**, *14*, 303–308.

(14) Bonnet, G.; Tyagi, S.; Libchaber, A.; Kramer, F. R. *Proc. Natl. Acad. Sci. U.S.A.* **1999**, *96*, 6171–6176.

(15) Tyagi, S.; Bratu, D. P.; Kramer, F. R. *Nat. Biotechnol.* **1998**, *16*, 49–53.

(16) Kostrikis, J. G.; Tyagi, S.; Mhlanga, M. M.; Ho, D. D.; Kramer, F. R. *Science (Washington, D.C.)* **1998**, *279*, 1228–1229.

(17) Sauer, M.; Han, K.-T.; Müller, R.; Nord, S.; Schulz, A.; Seeger, S.; Wolfrum, J.; Arden-Jacob, J.; Deltau, G.; Marx, N. J.; Drexhage, K.-H. *J. Fluoresc.* **1995**, *5*, 247–261.

(18) Lieberwirth, U.; Arden-Jacob, J.; Drexhage, K. H.; Herten, D. P.; Müller, R.; Neumann, M.; Schulz, A.; Siebert, S.; Sagner, G.; Klingel, S.; Sauer, M.; Wolfrum, J. *Anal. Chem.* **1998**, *70*, 4771–4779.

(19) Arden-Jacob, J. Ph.D. Thesis, Universität-Gesamthochschule Siegen, 1992.

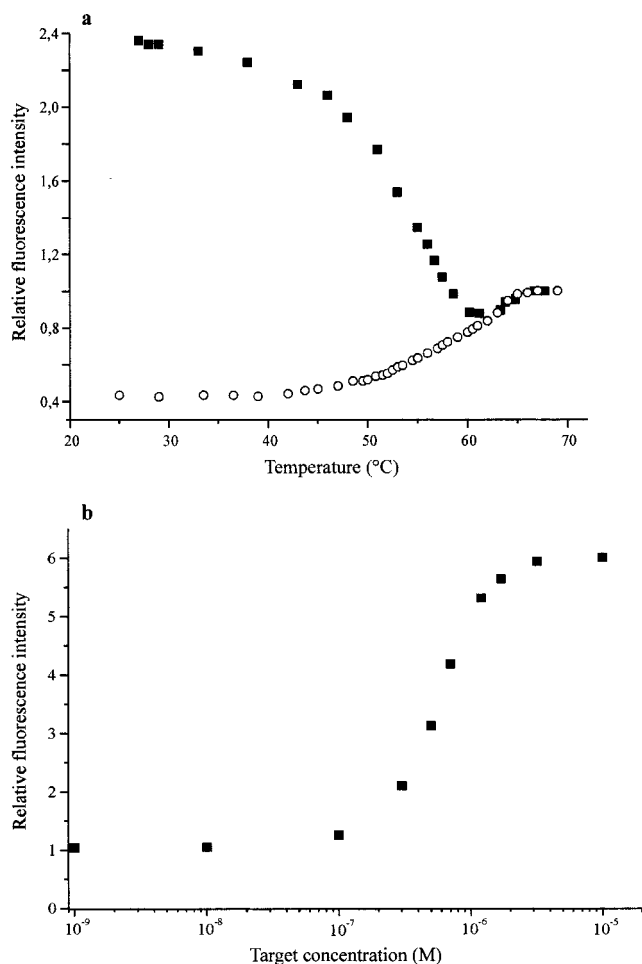


Figure 2. (a) Thermal denaturation profile of a  $10^{-7}$  M solution of smart probes in 100 mM tris-borate buffer (pH 7.4) containing 140 mM NaCl and 5 mM  $\text{MgCl}_2$  in the absence (open circles) and presence (solid squares) of a 10-fold excess of complementary target sequence. Fluorescence intensities were measured with a conventional spectrometer at 680 nm ( $\lambda_{\text{exc}} = 650$  nm) and normalized to a value of 1.00 at 67 °C. (b) Relative fluorescence intensity of a 50 nM solution of smart probes in 100 mM tris-borate buffer, 140 mM NaCl, 5 mM  $\text{MgCl}_2$  (pH 7.4) in the presence of varying concentrations of complementary target sequence ( $10^{-5}$ – $10^{-9}$  M). Using a conventional fluorescence spectrometer ( $\lambda_{\text{exc}} = 650$  nm,  $\lambda_{\text{em}} = 680$  nm), target concentrations down to  $10^{-7}$  M can be easily determined by the measured relative fluorescence intensity.

(25-mer, 5'-CCC CTA GTA GTT CCT CAC AGG GGG G-3'; 24-mer, 5'-ATT CCC TGT GAG GAA CTA CTA TTT-3'; d(C)<sub>18</sub>; d(G)<sub>30</sub>) were custom-synthesized by Carl Roth GmbH (Karlsruhe, Germany). The 25-mer and d(C)<sub>18</sub> oligonucleotide were modified at their termini using 5'-amino-modifier C<sub>6</sub>. The coupling reactions were carried out as follows. Twenty nanomoles of the 25-mer oligonucleotide was dissolved in 10  $\mu\text{L}$  of sterile water, and the following reagents were added in order: 25  $\mu\text{L}$  of *O*-(5-norbornene-2,3-dicarboximido)-*N,N,N,N*-tetramethyluronium tetrafluoroborate (100 mg/mL dimethylformamide), 20  $\mu\text{L}$  of the carboxyoxazine JA242 (5 mg/mL dimethylformamide), and 5  $\mu\text{L}$  of diisopropylethylamine. The solution was incubated for 15–20 h at room temperature in the dark. Labeled oligonucleotides were purified by reversed-phase (RP18 column) HPLC (Beckmann Instruments Inc., Fullerton, CA) using a gradient of 0–75% acetonitrile in 0.1 M aqueous triethylammonium acetate. Reaction

yields of 10–50% were achieved. Purified oligonucleotides were dissolved in 100 mM phosphate-buffered saline (PBS) (pH 7.4) containing 5 mM  $\text{MgCl}_2$ .

To investigate the absorption characteristics and to adjust the dye-labeled oligonucleotide concentration, we used the UV–visible spectrometer Lambda 18 (Perkin-Elmer, Foster City, CA). All experiments are done at 25 °C unless otherwise stated.

Steady-state fluorescence was measured in standard quartz cuvettes with a LS100 spectrometer (PTI, Canada). Corrected fluorescence spectra were obtained with a high-pressure xenon flash lamp as the excitation source at 635 nm. Relative fluorescence intensities and quantum yields were determined from the areas under the fluorescence spectra divided by their absorption intensity at 635 nm. To avoid reabsorption and reemission effects the concentration was kept strictly below 1.0  $\mu\text{mol/L}$  in all solutions.

Ensemble fluorescence lifetimes ( $10^{-8}$  M) were measured at the emission maximum using the technique of time-correlated single-photon counting (TCSPC) with an IBH spectrometer (model 5000MC; Glasgow, Scotland). As the excitation source, a pulsed laser diode emitting at 635 nm with a repetition rate of 1 MHz and a pulse length of 200 ps (fwhm) was used. To exclude polarization effects, the fluorescence was observed under the magic angle (54.7°). The decay parameters were determined by least-squares deconvolution, and their quality was judged by the reduced  $\chi^2$  values, the randomness of the weighted residuals, and the autocorrelation function. In cases in which a monoexponential model was not sufficient to describe the measured decay, a multiexponential model was used to fit the decay

$$I(t) = I(0) \sum a_i \tau_i \quad (1)$$

where  $a_i$  are the pre-exponential factors describing the ratio of the excited species ( $\sum a_i = 1$ ), and  $\tau_i$  are the corresponding lifetimes.

For enzymatic digestion of oligonucleotides Bal-31, exonuclease (New England BioLabs Inc., Schwalbach, Germany) was used. Bal-31 exonuclease degrades both 3' and 5' termini of duplex DNA without generating internal scissions. In addition, Bal-31 exonuclease is a highly specific single-stranded endonuclease which cleaves at nicks, gaps, and single-stranded regions of duplex DNA and RNA.<sup>20,21</sup> Digestion experiments were performed in standard quartz cuvettes using 500  $\mu\text{L}$  of a  $5 \times 10^{-7}$  M solution of the smart probe dissolved in nuclease buffer containing 300 mM NaCl, 10 mM Tris-HCl, 6 mM  $\text{CaCl}_2$ , 6 mM  $\text{MgCl}_2$ , 0.5 mM EDTA (pH 8.0) at 25 °C. Enzymatic cleavage was started upon addition of 1  $\mu\text{L}$  of undiluted Bal-31 exonuclease solution (1 Units). Thermal denaturation profiles in the presence or absence of complementary target sequence were measured in standard quartz cuvettes in 100 mM tris-borate buffer (pH 7.4) containing 140 mM NaCl and 5 mM  $\text{MgCl}_2$  using the LS100 spectrometer. The temperature was increased in various steps from 25 to 70 °C, with each step lasting 10 min prior to the fluorescence measurement, respectively.

**Single-Molecule Experiments.** The experimental setup for single-molecule experiments consists essentially of a standard

(20) Gray, H. B. *Nucleic Acids Res.* **1975**, *2*, 1459–1492.

(21) Legerski, R. J. *Nucleic Acids Res.* **1978**, *5*, 1445–1463.

inverse fluorescence microscope and is described in more detail in the literature.<sup>38,40</sup> A pulsed-diode laser emitting at 634 nm (PDL 800; Picoquant, Berlin, Germany) served as the excitation source. This laser system provides light pulses with a duration of less than 100 ps full width at half-maximum (fwhm) at a repetition rate of 64 MHz. The collimated laser beam was coupled into an oil-immersion objective (100× NA = 1.4; Nikon, Japan) by a dichroic beam splitter (645DRLP; Omega Optics, Brattleboro, VT). The average laser power was adjusted with neutral density filters to be 500 μW at the sample. The fluorescence signal was collected by the same objective, filtered by a band-pass filter (675RDF50; Omega Optical, Brattleboro, VT), and imaged onto a 100-μm pinhole oriented directly in front of an avalanche photodiode (AQ-131; EG&G Optoelectronics, Canada). The detector signal was registered by a PC plug-in card for time-correlated single-photon counting (TCSPC) (SPC-430; Becker&Hickl, Berlin, Germany). With this card, a minimum collection (integration) time of 150 μs per decay curve (64 channels) for a gap-free measurement is possible.<sup>22</sup> The instrument response function of the entire system was determined to be 420 ps. From the data of the TCSPC card, multichannel-scalar (MCS) traces were generated. For this, all photons of a decay curve were added up to a bin of the MCS trace. The raw data are shown without modification by any filtering algorithm. The solutions for single-molecule experiments were prepared by diluting a stock solution containing smart probe molecules (10<sup>-6</sup> M) with the appropriate amount of buffer (100 mM tris-borate, pH 7.4, containing 140 mM NaCl and 5 mM MgCl<sub>2</sub>) down to the required concentration of 5 × 10<sup>-10</sup> M. The samples were transferred onto a microscope slide with a small depression and covered by a cover glass.

The fluorescence decay time of single-molecule events was determined by a maximum likelihood estimator (MLE) using the following relation:<sup>23,24</sup>

$$\frac{\omega}{1 - e^{-\omega/\tau}} - \frac{m\omega}{e^{m\omega/\tau} - 1} = \frac{\sum_{i=1}^m i\omega N_i}{N} \quad (2)$$

Here,  $N$  is the number of photon counts taken into account, and the sum runs over the  $m$  bins of width  $\omega$ , with the  $i$ th bin containing  $N_i$  counts. Because of the low photon count statistics in single-molecule experiments, a deconvolution procedure of the data is complicated. To estimate the fluorescence decay time,  $\tau$ , only a portion of  $m$  channels of width  $\omega$  were used. The parameters used, in particular, are  $m = 53$  and  $\omega = 0.195$  ns. Typically, the data window with a width of about 10 ns started 400 ps behind the peak maximum of the decay curve. Equation 2, which holds only for monoexponential decays, disregarding the convolution with the laser pulse, was numerically solved with respect to the fluorescence decay time  $\tau$  using Newton's algorithm. The experimental standard deviation  $\sigma_{\text{exp}}$  was obtained from the distribution of the calculated fluorescence decay times.

## RESULTS AND DISCUSSION

### Design and Spectroscopic Characteristics of Smart Probes.

Fluorescent dye molecules that are influenced by the environment can act as molecular probes, i.e., they exhibit information about neighboring groups and changes in the polarity of the micro-environment. Hence, this property might also be useful to probe the presence of specific nucleosides in the nearby neighborhood of the dye. Seidel and co-workers first reported on nucleobase-specific fluorescence quenching of coumarin dyes by neighboring DNA bases.<sup>25</sup> They suggested the use of a so-called "intelligent" coumarin dye (coumarin-120) with nucleobase-specific fluorescence decay times for the realization of a new one-lane one-dye concept for DNA sequencing.

Previously, we found that also rhodamine and oxazine derivatives are influenced by DNA bases. Upon close contact with guanosine residues, the dye is more or less efficiently quenched by the DNA nucleoside guanosine.<sup>17,18</sup> Covalent linking of these dyes to oligonucleotides containing guanosine residues results in a diminished fluorescence quantum yield and decay time dependent on the distance between the guanosine residue and the fluorescent dye.<sup>26</sup> In addition, we could demonstrate that the fluorescence kinetics of the dye are influenced mainly when the guanosine residue is located in the near vicinity of the dye.<sup>27</sup> Recently,<sup>28,29</sup> this observation has been supported by several other groups and used to study conformational fluctuations in DNA oligonucleotides at the single-molecule level by time-resolved fluorescence detection.<sup>27,30–32</sup> As in the case of stilbene-labeled hairpin oligonucleotides with dC-dG stems, a photoinduced electron-transfer reaction from the guanine ground state to the excited rhodamine or oxazine singlet state provides a plausible mechanism for fluorescence quenching.<sup>33</sup> The difference in behavior of neighboring dG compared with dA, dT, or dC bases can be attributed to the lower oxidation potential of dG versus that of dA or the pyrimidine bases dT and dC.<sup>17,25,34</sup>

Besides the monitoring of the dynamical behavior of DNA oligonucleotides, the quenching influence of guanosine residues on the attached reporter dye might be a powerful tool to probe the local DNA sequence in double- or single-stranded DNA. To

- (22) Becker, W.; Hickl, H.; Zander, C.; Drexhage, K. H.; Sauer, M.; Siebert, S.; Wolfrum, J. *Rev. Sci. Instrum.* **1999**, *70*, 1835–1841.
- (23) Tellinghuisen, J.; Wilkerson, C. W., Jr. *Anal. Chem.* **1993**, *65*, 1240–1246.
- (24) Soper, S. A.; Legendre, B. L., Jr. *Appl. Spectrosc.* **1994**, *48*, 400–405.
- (25) Seidel, C. A. M.; Schulz, A.; Sauer, M. *J. Phys. Chem.* **1996**, *100*, 5541–5553.
- (26) Sauer, M.; Drexhage, K. H.; Hertel, D. P.; Lieberwirth, U.; Müller, R.; Nord, S.; Schulz, A.; Siebert, S.; Wolfrum, J. In *Near-Infrared Dyes for High Technology Applications*; Daehne, S., et al., Eds.; Kluwer Academic Publishers: Dordrecht, The Netherlands, 1998; pp 57–85.
- (27) Sauer, M.; Drexhage, K. H.; Lieberwirth, U.; Müller, R.; Nord, S.; Zander, C. *Chem. Phys. Lett.* **1998**, *284*, 153–163.
- (28) Vámosi, G.; Gohlke, C.; Clegg, R. M. *Biophys. J.* **1996**, *71*, 972–994.
- (29) Widengren, J.; Dapprich, J.; Rigler, R. *Chem. Phys.* **1997**, *216*, 417–426.
- (30) Edman, L.; Mets, Ü.; Rigler, R. *Proc. Natl. Acad. Sci. U.S.A.* **1996**, *93*, 6710–6715.
- (31) Jia, Y.; Sytnik, A.; Li, L.; Vladimirov, S.; Cooperman, B. S.; Hochstrasser, R. M. *Proc. Natl. Acad. Sci. U.S.A.* **1997**, *94*, 7932–7936.
- (32) Eggeling, C.; Fries, J. R.; Brand, L.; Günther, R.; Seidel, C. A. M. *Proc. Natl. Acad. Sci. U.S.A.* **1998**, *95*, 1556–1561.
- (33) Lewis, F. D.; Wu, T.; Zhang, Y.; Letsinger, R. L.; Greenfield, S. R.; Wasielewski, M. R. *Science (Washington, D.C.)* **1997**, *277*, 673–676.
- (34) Steenken, S.; Jovanovic, S. V. *J. Am. Chem. Soc.* **1997**, *119*, 617–618.
- (35) Marras, S. A. E.; Kramer, F. R.; Tyagi, S. *Genet. Anal.* **1999**, *14*, 151–156.
- (36) Nie, S.; Zare, R. N. *Annu. Rev. Biophys. Biomol. Struct.* **1997**, *26*, 567–596.
- (37) Ambrose, W. P.; Goodwin, P. M.; Jett, J. H.; Van Orden, A.; Werner, J. H. Keller, R. A. *Chem. Rev.* **1999**, *99*, 2929–2957.
- (38) Sauer, M.; Arden-Jacob, J.; Drexhage, K. H.; Göbel, F.; Lieberwirth, U.; Mühlegger, K.; Müller, R.; Wolfrum, J.; Zander, C. *Bioimaging* **1998**, *6*, 14–24.
- (39) Schaffer, J.; Volkmer, A.; Eggeling, C.; Subramanian, V.; Striker, G.; Seidel, C. A. M. *J. Phys. Chem. A* **1999**, *103*, 331–336.
- (40) Sauer, M.; Angerer, B.; Han, K.-T.; Zander, C. *Phys. Chem. Chem. Phys.* **1999**, *1*, 2471–2477.

Table 1. Spectroscopic Data of the Free Dye JA242 and the d(C)<sub>18</sub> Conjugate in the Presence and Absence of a 100-Fold Excess of d(G)<sub>30</sub> in 100 mM Tris-Borate Buffer (pH 7.4) Containing 140 mM NaCl and 5 mM MgCl<sub>2</sub><sup>a</sup>

	$\lambda_{abs}$ (nm)	$\lambda_{em}$ (nm)	$\Phi_{f,rel}$	$\tau_1$ (ns)/ $a_1$	$\tau_2$ (ns)/ $a_2$	$\tau_3$ (ns)/ $a_3$	$\chi^2$
JA242	664	682	0.91	1.93/1.00			0.996
JA242-NH-C <sub>6</sub> -d(C) <sub>18</sub>	670	685	1.00	1.95/0.12	3.13/0.88		1.002
JA242-NH-C <sub>6</sub> -d(C) <sub>18</sub> + G <sub>30</sub>	673	686	0.21	0.23/0.23	1.11/0.42	2.67/0.35	1.032

<sup>a</sup> The ensemble fluorescence decay times,  $\tau_i$ , were measured with a standard spectrometer for TCSPC using a pulsed diode laser as the excitation source (4096 channels at 12.5 ps, 10 000 photons in the maximum channel). The relative fluorescence quantum yield,  $\Phi_{f,rel}$  of JA242-NH-C<sub>6</sub>-d(C)<sub>18</sub> was set to 1.00.

test this principle, we coupled the oxazine dye JA242 covalently to the 5' end of d(C)<sub>18</sub>. As can be seen in Table 1, the oxazine derivative JA242 exhibits monoexponential fluorescence kinetics. On the other hand, the conjugate JA242-NH-C<sub>6</sub>-d(C)<sub>18</sub> shows a slightly increased fluorescence quantum yield accompanied by a main fluorescence component with a longer decay time. Because of the observed bathochromic shifts in absorption and emission maxima (Table 1), we assume that fluorescent ground-state complexes are formed between the dye and the hydrophobic part of the nucleotides. After addition of an excess of d(G)<sub>30</sub>, the fluorescence quantum yield decreases drastically. The fluorescence kinetics indicate the presence of at least three decay times: two shorter and one longer decay component compared with the decay time of the free dye. In the conjugate (JA242-C<sub>6</sub>-d(C)<sub>18</sub>) the dye is coupled through a C<sub>6</sub>-aminolinker to the 5' end of the d(C)<sub>18</sub> chain. As a result of the conformational flexibility of the linker and the tendency of nonpolar species, such as rhodamine and oxazine dyes, to aggregate in water so as to decrease the hydrocarbon-water interfacial area, an interaction between the oxazine and the hydrophobic part of the nucleotides is possible. As observed in single-molecule experiments,<sup>27,30–32</sup> the short fluorescence decay times of the hybridized conjugate result from ground-state complexes and interactions with guanosine residues in the complementary strand, whereas the longer decay component represents a distribution of decay times resulting from interactions between the dye and the cytosine residues and noninteracting dye molecules. The existence of two different quenched compounds indicates that the dye adopts at least two favored conformations with respect to the guanosine residues in the complementary DNA strand.

To use the specific fluorescence quenching of oxazine dyes by guanosine residues to probe the sequence of a target DNA, we synthesized single-stranded oligonucleotides that possess a 13-nucleotide loop and a 5-nucleotide and a 7-nucleotide arm, respectively (Figure 1). The loop and parts of the guanosine-containing arm sequence consist of a probe sequence that is complementary to a sequence in the target, whereas the stem is formed by annealing of complementary cytosine and guanosine sequences, which are unrelated to the target sequence. The probe sequence includes 3 of the 6 guanosine residues of the arm sequence to increase the hybridization kinetics, especially at lower temperatures. The complementary arms are so close to one another in the hairpin structure that the fluorescent dye JA242 (attached at the cytosine arm) is efficiently quenched by the complementary guanosine residues. As shown in Figure 1, upon addition of a 100-fold excess of target sequence to a solution of so-called smart probes, a longer and more stable hybrid is formed

with the target sequence. Thus, the measured fluorescence intensity increases about 6-fold. To check the hybridization efficiency, we digested the smart probes by addition of Bal-31 exonuclease. After about 150 s, all smart probe molecules are digested, which results again in a 6-fold increased fluorescence intensity (data not shown).

Figure 2a shows thermal denaturation profiles of smart probes in the absence and presence of a 100-fold excess of complementary single-stranded target sequence. In the absence (open circles) of target molecules, the fluorescent dye and the guanosine residues are held in close proximity to each other by the hairpin stem at low temperatures. However, with increasing temperature, the double-stranded stem is destabilized, separating the dye from the guanosine residues. Thus, the fluorescence intensity increases. The transition from the helical structure to a random coil configuration occurred at 58 °C.

In the presence of complementary target molecules (solid squares in Figure 2b), fluorescence intensity decreases with increasing temperature followed by a slight increase in fluorescence at temperatures above 60 °C. At low temperatures, smart probes spontaneously form probe–target duplexes that are more stable than the hairpin stem. As the temperature is raised, a transition to the quenched hairpin stem occurs at 53 °C. Therefore, the fluorescence intensity decreases drastically. As the temperature is increased further, the quenched hairpin-stems melt into unquenched random coils.

As demonstrated in Figure 3b, the spontaneous formation of the more stable probe–target duplex can be used to detect the presence of a specific target sequence in the concentration range 10<sup>−5</sup> to 10<sup>−7</sup> M using standard fluorescence spectrometers. In addition, hairpin oligonucleotides are considerably more specific than the corresponding linear probes.<sup>15,35</sup>

**Experiments at the Single-Molecule Level.** While ensemble measurements yield only information on average properties, single-molecule experiments allow the identification of individual characteristics, i.e., identification of subpopulations, in a heterogeneous mixture.<sup>4,36–42</sup> This feature might also be helpful for the discrimination of quenched smart probes and fluorescent probe–target duplexes. As can be seen in part a of Figure 3, only a few smart probes exhibit sufficient fluorescence intensities for their unequivocal detection at the single-molecule level. The highest fluorescence burst intensities reach count rates of about 40 kHz.

- (41) Ha, T.; Ting, A. Y.; Liang, J.; Caldwell, W. B.; Deniz, A. A.; Chemla, D. S.; Schultz, P. G.; Weiss, S. *Proc. Natl. Acad. Sci. U.S.A.* **1999**, *96*, 893–898.  
(42) Deniz, A. A.; Dahan, M.; Grunwell, J. R.; Ha, T.; Faulhaber, A. E.; Chemla, D. S.; Weiss, S.; Schultz, P. G. *Proc. Natl. Acad. Sci. U.S.A.* **1999**, *96*, 3670–3675.

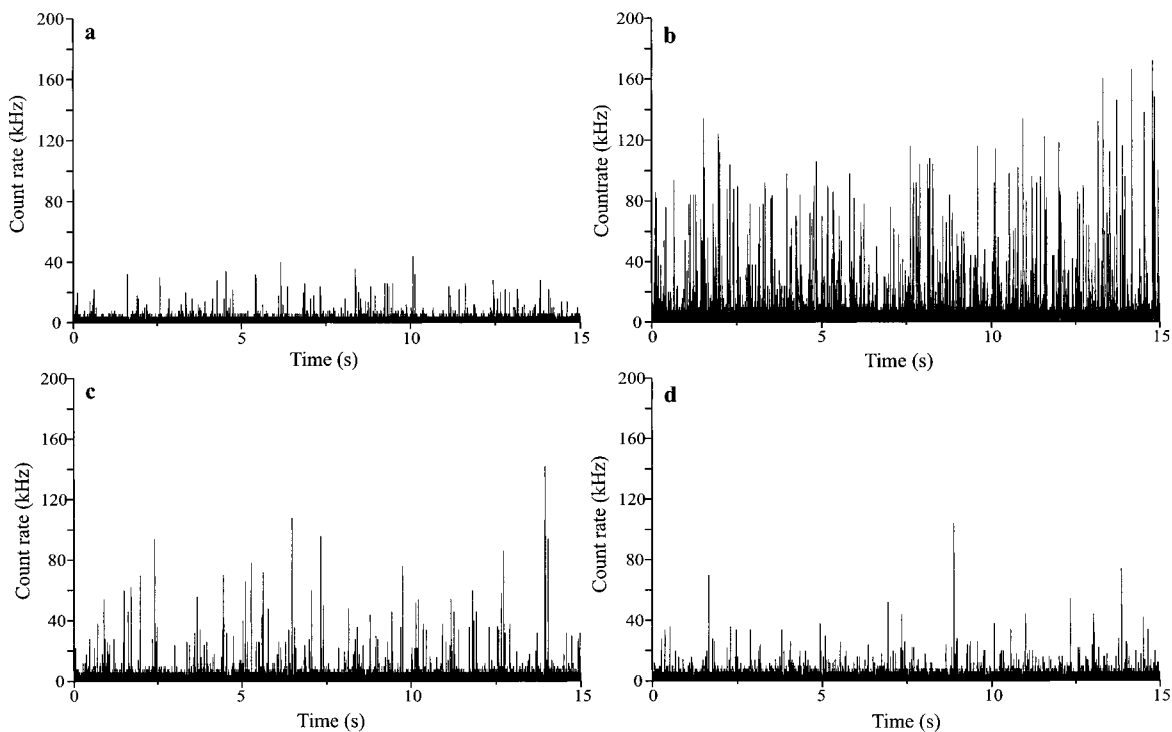


Figure 3. Fluorescence signals observed from a  $5 \times 10^{-10}$  M solution of smart probe in 100 mM tris-borate buffer (pH 7.4), 140 mM NaCl, 5 mM  $\text{MgCl}_2$  in the absence and presence of different concentrations of complementary target sequence. (a) no target sequence, (b)  $10^{-7}$  M target, (c)  $10^{-9}$  M target, (d)  $10^{-12}$  M target. The data were binned into 0.5-ms time intervals.

The low number of detected fluorescence bursts indicates that the fluorophore is efficiently quenched by guanosine residues in almost all smart probes.

Upon addition of a 100-fold excess of complementary target sequence (part b of Figure 3), smart probes form a stable probe–target duplex that exhibits an increased fluorescence quantum yield. As in ensemble measurements, the average count rate increases about 6-fold. Furthermore, the number of fluorescence bursts with high count rate increases significantly. This experiment clearly demonstrates that most of the smart probes exhibit fluorescence quantum yields that prevent their detection at the single-molecule level. As indicated in parts c and d of Figure 3, even upon addition of lower amounts of target DNA the data indicate small differences in burst size and number of detected bursts with count rates  $> 30$  kHz.

To find an optimal way for discrimination between smart probes and probe target duplexes all single-molecule bursts above a certain threshold were analyzed by a burst recognition procedure. With the used setup, an average background of 1 kHz was obtained in the described solvent. To suppress the background efficiently, only bursts with count rates higher than 30 kHz were utilized. The starting and end points of a burst were defined by a count rate of 10 kHz. In case two count rate maxima fall into the same time interval, we split such a burst at the minimum count rate between the maxima. Besides the burst rate (number of fluorescence bursts per time), we get three additional parameters for each burst: (a) the number of detected photon counts per burst (burst size), (b) the length of the burst (burst duration), and (c) the fluorescence decay time calculated with the MLE algorithm.

For the following statistics, we used single-molecule data collected from smart probes in the absence and presence of a

100-fold excess of target sequence. During 200 s we identified 145 fluorescence bursts in the absence of a complementary target sequence and 2107 fluorescence bursts with count rates higher than 30 kHz in the presence of such a sequence, i.e., burst rates of 0.73 and 10.94 Hz, respectively. In other words, a 15-fold increase in the defined burst rate upon specific hybridization to the target DNA was found. Figure 4 shows the corresponding distributions in burst size, burst duration, and fluorescence decay time. As expected for single-molecule measurements in an open detection volume, most analyte molecules cross the detection volume at the edge. Hence, most fluorescence bursts have a small size and the burst-size frequency increases toward smaller sizes.<sup>37,40</sup> However, as can be seen from the normalized burst-size distributions shown in Figure 4a, most smart probes exhibit burst sizes well below 50 counts. On the other hand, also the burst length, i.e., the diffusional motion of a single molecule, and the fluorescence kinetics of the excited state of the fluorophore might reflect changes in the microenvironment of individual molecules. The slightly prolonged burst durations of hybridized smart probes (part b of Figure 4) indicate different diffusional motion of spherical smart probes and more stretched target hybrids. In addition, the higher burst rate in the presence of a 100-fold excess of target DNA increases the probability of coincidences of two-molecule events.

Part c of Figure 4 shows the resulting distribution of measured fluorescence decay times of each recognized burst. The Gaussian fits reveal two different fluorescence decay times for smart probes of  $1.81 \pm 0.34$  ns in the absence and  $2.89 \pm 0.53$  ns in the presence of complementary target DNA. The relatively long fluorescence decay time found in the absence of target DNA might be explained by at least three facts: (a) we used a MLE algorithm without deconvolution from the laser pulse that disregards multiexponen-

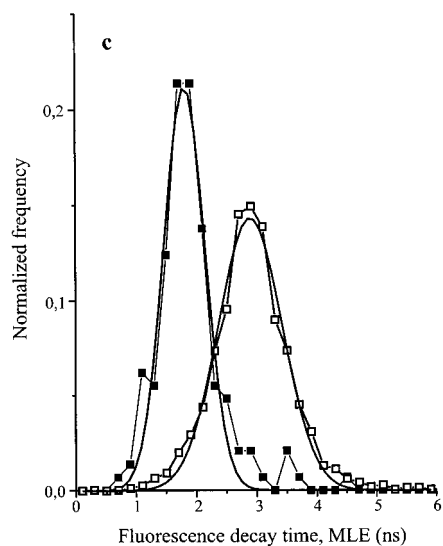
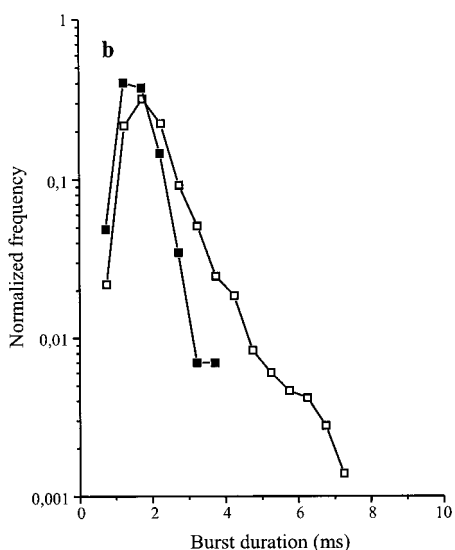
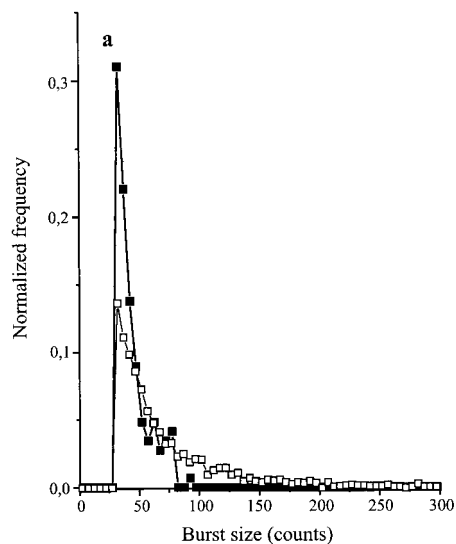


Figure 4. (a) Normalized burst sizes, (b) burst durations (semilog plots), and (c) fluorescence decay time distributions of photon bursts detected within 200 s of a  $5 \times 10^{-10}$  M solution of smart probes in the absence (solid squares) and in the presence (open squares) of a 100-fold excess of target DNA in 100 mM tris-borate buffer, 140 mM NaCl, 5 mM MgCl<sub>2</sub> (pH 7.4).

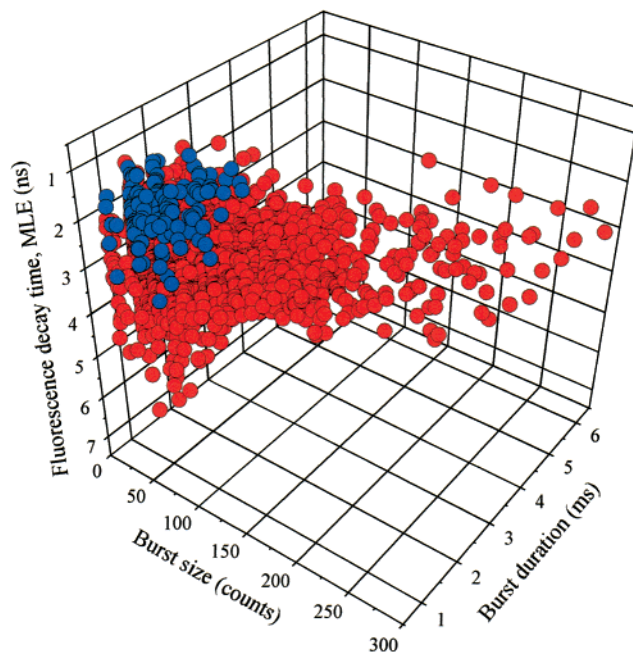


Figure 5. Three-dimensional plot of burst size, burst duration, and fluorescence decay time of the data shown in Figure 4. Nearly all smart probes exhibit burst sizes smaller than 50 counts, burst durations below 2.0 ms, and fluorescence decay times shorter than 2.4 ns in the absence of target DNA (blue circles). On the other hand, upon addition of a 100-fold excess of complementary target sequence (red circles), about 50% of detected fluorescence bursts with count rates higher than 30 kHz are located outside of a 3D area defined by a burst size of  $< 50$  counts, a burst duration of  $< 2.0$  ms, and a fluorescence decay time  $\tau < 2.4$  ns.

tial fluorescence kinetics, i.e., the long decay-time component (see Table 1) dominates the calculated decay time, (b) efficiently quenched smart probes with very short decay time withdraw themselves from a detection at the single-molecule level, and (c) due to the conformational flexibility of the used C<sub>6</sub> linker, the fluorophore might adopt different configurations with respect to the nucleotides in the complementary DNA strand of the hairpin system, thus changing the observed fluorescence decay time during the transition through the detection volume.<sup>27,32</sup> Strong fluorescence intensity jumps during the transition through the detection volume might also decrease the observed burst duration of smart probes. Nevertheless, differences in fluorescence decay time can be used as an efficient additional parameter to discriminate between smart probes and probe–target duplexes.

Figure 5 summarizes the obtained information. More than 97% of the detected bursts exhibit a burst size smaller than 50 counts, a burst duration below 2.0 ms, and a fluorescence decay time shorter than 2.4 ns (intersection of the two Gaussians in Figure 4c) in the absence of target DNA. On the other hand, in the presence of a 100-fold excess of target DNA, about 50% of all identified fluorescence bursts are located outside the defined 3D area. The obtained result, i.e., a  $\sim 20$ -fold increase in the portion of bursts located outside the defined 3D area, is comparable with the factor obtained from simple-burst-rate measurements. However, as can be seen by the black squares in Figure 6, at lower target DNA concentrations, the detection accuracy decreases drastically. The detection of target DNA concentrations below  $10^{-9}$  M is prevented if only fluorescence intensity information is used.

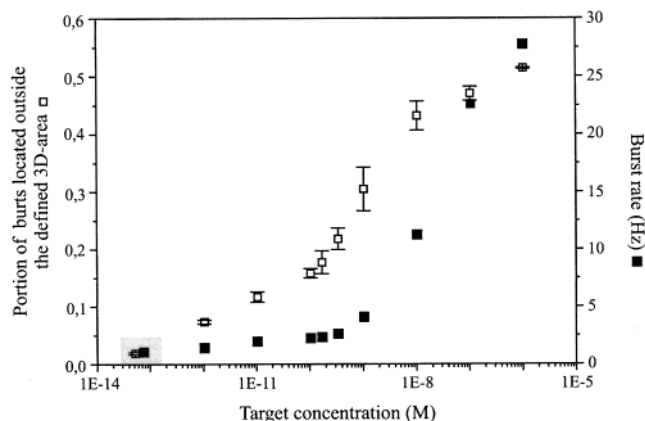


Figure 6. Detected burst rate and portion of fluorescence bursts located outside the defined 3D area measured during 200 s as a function of complementary target DNA concentration. Measurements were performed in 100 mM tris-borate buffer, 140 mM NaCl, 5 mM MgCl<sub>2</sub> (pH 7.4). The error bars result from three independent measurements. The two data points with gray background give the values for smart probes in the absence of target DNA.

At concentrations below the nanomolar range, the use of additional information, i.e., burst duration and fluorescence decay time, improves the discrimination accuracy significantly (see open squares in Figure 6).

The analysis uses the portions of bursts that are located outside a specific 3D area which is defined by the following criteria: (a) burst size > 50 counts, (b) burst duration < 2.0 ms, and (c) fluorescence decay time  $\tau$  < 2.4 ns. Hence, the method is independent of the overall number of detected bursts (burst rate). By the use of this analysis, even target DNA concentrations of 10<sup>-12</sup> M are easily recognized in a homogeneous assay by a 3-fold-increased portion of fluorescence bursts located outside the defined 3D area.

## CONCLUSIONS

We have synthesized new DNA probes for highly specific recognition of complementary target DNA in a homogeneous

assay. The new smart probes consist of a dye-labeled stem-loop structure that is released upon specific hybridization to the target sequence. In contrast to double-labeled molecular beacons, the synthesis of smart probes is drastically simplified. In addition, incompletely labeled probes do not contribute to the measured signal as in the case of molecular beacons. Especially in applications that require higher identification sensitivities, photodestruction of the acceptor chromophore and subsequent increase of donor fluorescence intensity might render the unequivocal identification of hybridization events to target DNA more difficult. In contrast, unlabeled or photobleached fluorophores do not contribute to the measured signal in the case of the smart probe concept.

To further increase the identification sensitivity, a multidimensional analysis strategy has been developed at the single-molecule detection level. The strategy takes advantage of the fact that individual smart probes exhibit several different characteristics after hybridization to the target sequence. Besides higher burst sizes and longer burst durations, probe–target duplexes exhibit a significantly increased fluorescence decay time. This enables the efficient discrimination between smart probes and hybridized probe–target duplexes down to target concentrations of 10<sup>-12</sup> M, i.e., identification of probe–target duplexes in the presence of a 200-fold excess of smart probe molecules.

## ACKNOWLEDGMENT

We thank J. Wolfrum for stimulating discussion, C. Zander for technical assistance, and K.-H. Drexhage for generous disposal of the oxazine derivative JA242. Financial support by the Volkswagen-Stiftung (Grant I/74 443) and the Bundesministerium für Bildung, Wissenschaft, Forschung, und Technologie (Grant 11864 BFA082) is gratefully acknowledged.

Received for review January 5, 2000.

AC0000240